Animal Cells and Systems
Vol. 16, No. 5, October 2012, 357–365

Taylor & Francis
Taylor & Francis Group

The effects of circadian disturbances induced by night shifts on the mouse peripheral tissues

Dong-Hyun Seo[a], Han-Sung Kim[a], Chang-Yong Ko[b,c], Jürgen Schreiber[b,c], Yeong-Su Jang[d] and Kiho Bae[d]*

[a]*Department of Biomedical Engineering, Institute of Medical Engineering, Yonsei-Fraunhofer Medical Device Lab, Yonsei University, Wonju 220-710, Korea;* [b]*Structural and Medical Health Monitoring, Fraunhofer Institute for Nondestructive Testing IZFP, Dresden 01109, Germany;* [c]*Yonsei-Fraunhofer Medical Device Lab, Wonju 220-710, Korea;* [d]*Division of Biological Science and Technology, Yonsei-Fraunhofer Medical Device Lab, Yonsei University, Wonju 220-710, Korea*

(*Received 15 March 2012; received in revised form 7 June 2012; accepted 14 June 2012*)

We have examined the effect of circadian disturbances induced by night shifts (NSs) on the phenotypes of the tibiae and abdominal adipose tissues (ADTs) in a mouse model by using *in vivo* micro-computed tomography (micro-CT). We found that the volumes of total and visceral ADTs in the night-shifted group of mice were significantly larger (69 and 92%, respectively) than those in the control. The mean polar moment of inertia, cross-sectional thickness, and bone mineral density of the cortical bone in the night-shifted group of mice were less (13, 5, and 3%, respectively) than those in the control. Moreover, the volume and the thickness of growth plates (GPs) of the tibiae in the night-shifted mice were significantly smaller (22 and 20%, respectively) than those in the control. Taken together, our results indicate that disturbances in the mouse circadian rhythms induced by NSs affect the morphological characteristics of cortical bone, the volume and the thickness of GPs, and the volume of ADTs.

Keywords: circadian rhythm; *in vivo* micro-CT; tibiae; adipose tissues

1. Introduction

Organisms have evolved biological rhythms in response to periodic changes in their environments. The biological rhythm is a representative of the adaptation to synchronize the activities of organisms to their environment such as day/night cycles (Robert and Moore 1997). Among these rhythms, the circadian rhythm is an example with about 24-h period lengths that is closely related to the sleep/activity cycles and a number of biological activities in the organism (Bunger et al. 2000; Reppert and Weaver 2001; Lee and Kim 2012).

Based on many studies, the suprachiasmatic nucleus (SCN) of the ventral hypothalamus in the mammalian brain is known for the primary region regulating circadian rhythms of endocrine activity, temperature, energy metabolism, and locomotion (Akiyama et al. 1999; Joo 2006; Zvonic et al. 2006; Francine et al. 2007). Circadian rhythms are controlled by exogenous factors (Zeitgeber; time giver) such as light, temperature, and feeding, with light being the most critical Zeitgeber. Indeed, the regulation of circadian rhythms is significantly affected by the exposure of light that is passed to the SCN via the retina (Joo 2006). Circadian rhythms are also present to maintain and regulate each organ-specific rhythm in peripheral tissues such as liver, kidney, and heart. The SCN functions as the central clock that synchronizes with the peripheral clocks (Akhtar et al. 2002; Francine et al. 2007; Hastings et al. 2007).

We human beings nowadays increasingly experience night shifts (NSs) due to irregular activities such as shift work (Lee et al. 2007; Sun et al. 2009). It has been reported that NS works create confusion in the circadian rhythm and lower the quantity and quality of sleep. Night shifts also cause physiological and endocrine dysfunction, which may lead to sleep, nervous, digestive or cardiovascular disorders, and may reduce the average lifespan (Lee et al. 2007; Sun et al. 2009). Furthermore, disturbance in circadian rhythms, especially for adolescents can cause imbalances in growth, inhibition of growth, and adolescent obesity (Zvonic et al. 2006).

Studies regarding how the NSs could induce disturbances in circadian rhythms have been conducted with human subjects and however, some studies revealed drawbacks in limited numbers of participants and durations (Francine et al. 2007). Moreover, other factors aside from NSs, such as light, eating, and waking time, may also cause disturbances in circadian rhythms because of the limitations of the experimental environment. For the reasons, it is difficult to obtain accurate results from studies of circadian rhythms in human subjects. Thus, many researchers have been adopted an animal model instead to obtain more reproducible and reliable results regarding the effects of disturbances in circadian rhythms.

Although several studies have examined the effects of circadian rhythm disruption on the ethology, physiology, and endocrinology of human subjects or animal models, there has not been more quantitative analysis and evaluation of the effect of NSs on the phenotypes of peripheral tissues such as bones (Francine et al. 2007; Lee et al. 2007; Sun et al.

*Corresponding author. Email: kbae@.yonsei.ac.kr

ISSN 1976-8354 print/ISSN 2151-2485 online

http://dx.doi.org/10.1080/19768354.2012.706639
http://www.tandfonline.com

2009). Therefore, in this study, we set out to determine and evaluate the effect of a NS-induced disturbance in circadian rhythms on the phenotypes of adipose tissues and cortical bones, tibiae in mice by using micro-computed tomography (micro-CT). Indeed, we could observe that the morphological characteristics of cortical bone, tibiae, and the volume of abdominal adipose tissues (ADTs) have been significantly altered after these mice were being exposed to NSs, the reversal of light/dark (LD) cycles.

2. Materials and methods

2.1. Animals

The animals used in the experiment were previously described (Bae et al. 2001). All procedures were performed under a protocol approved by the Institutional Animal Care and Use Committee (YWC-100303-1). Five-week-old male 129/sv mice (18.5–22.5 g) were randomly allocated into two groups, the normal (NOR, $n=7$) and the night shift (NS, $n=7$) group. The light in the mouse rack was controlled with an adjustable timer to regulate the sleep cycle. The NOR group of mice was continuously maintained under 12-h of light/12-h of dark cycles (lights-on at Zeitgeber time [ZT] 0 and lights-off at ZT12) for six weeks. The NS group was kept under LD cycles for weeks 0–2 and weeks 4–6 (lights-on at ZT0 and lights-off at ZT12), and under DL cycles (lights-off at ZT0 and lights-on at ZT12) for weeks 2–4 (Figure 1A).

2.2. RNA isolation, cDNA synthesis, and real-time PCR

Mouse liver samples were collected at every four hours starting ZT1 and total RNA was extracted from the livers using TRI reagent (Sigma, MO, USA). The PrimeScript 1st strand cDNA synthesis kit (TaKaRa Bio Inc., China) was used to synthesize cDNA from 1 μg of total RNA according to the manufacturer's instructions. Then, the PCR reactions were carried out using the StepOnePlus System (Applied Biosystems, CA, USA) according to the manufacturer's protocol, and the detection of fluorescent products was carried out at the end of the 72°C extension period. The initial amount of cDNA in each sample was

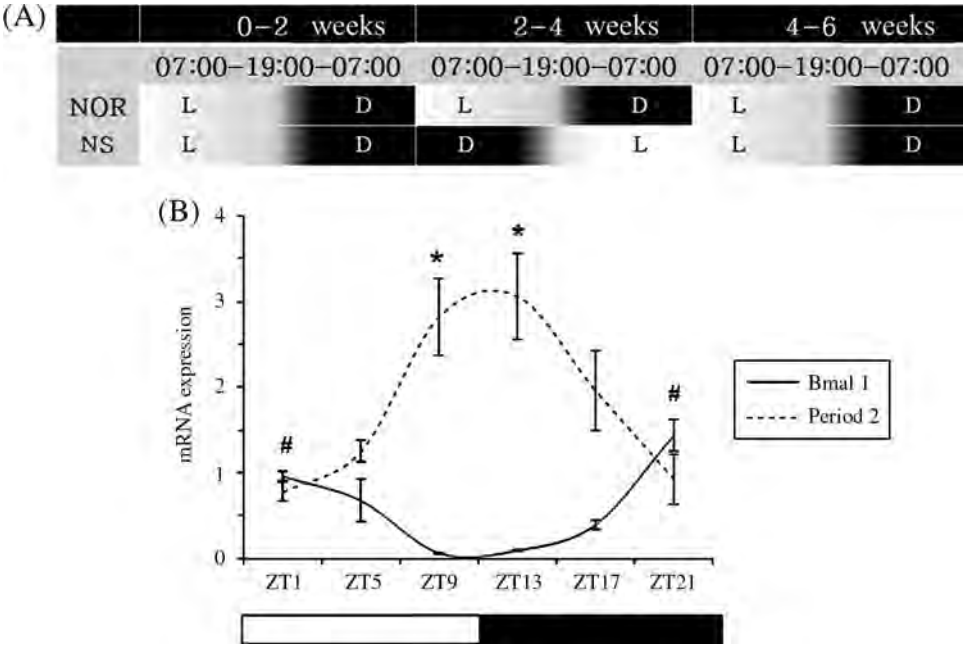

Figure 1. (A) A timetable showing the lighting regime for the experiment. Mice were randomly allocated into two groups, NOR (normal, $n=7$) and NS (night shift, $n=7$) group, and being exposed to different lighting schedules. The NOR mice were kept at 12-h of light (L)/12-h of dark (D) cycle for six weeks. For the NS group, the reverse LD cycles were applied to them for two weeks after two weeks of the entraining periods, and then they were being released back to normal lighting schedules for additional two weeks. (B) Temporal mRNA expression profiles of two canonical clock genes, *Bmal1* (solid line) and *Period2* (broken line), are shown as a line graph. Livers from wild-type mice entrained to 12-h:12-h LD cycles were collected at every four hours starting ZT1, and real-time PCR was performed using primers specific to *Bmal1* and *Period2*, respectively. Both mRNAs oscillates in a time-of-day specific manner, with anti-phasic to each other. The house-keeping gene *β-actin* was used as a constitutive control for normalization. The white and black bars below the graph represent 12-h of daytime and 12-h of darkness, respectively. All data are expressed as the mean ± SE. $^{\#}p<0.05$ for *Bmal1* and $*p<0.05$ for *Period2* among time points.

Table 1. Primer sequences used in the experiment.

Name of primer	Oligonucleotide sequence
Bmal1 forward	ATTCCAGGGGGAACCAGAG
Bmal1 reverse	CCCTCCATTTAGAATCTTCTTGC
Period2 forward	CGTGAAGAACGCGGATATGTTTG
Period2 reverse	AAGAATCTAAGCCGCTGCACACAC
β-*actin* forward	TTTTCCAGCCTTCCTTCTTG
β-*actin* reverse	TGTGTTGGCATACAGGTCTT

Note: The sequences are all written from 5′ to 3′ directions.

calculated using the $2^{-\Delta\Delta Ct}$ method (Livak and Schmittgen 2001). The housekeeping gene β-*actin* was used as a constitutive control for normalization. All samples were analyzed in three independent experiments and measured in triplicates in each experiment. The primer pairs used for PCR are listed in Table 1.

2.3. In vivo micro-CT

The tibiae and torsos (Lumbar 2–5, L2–L5) were scanned at 0 and 6 weeks using *in vivo* micro-CT, (Skyscan 1076, Skyscan N.V., Belgium). To immobilize mice during the scan, each mouse was anesthetized with ketamine (50 mg/kg) and xylazine (6 mg/kg) by intraperitoneal injection. The parameters used for scanning in the experiment are previously described (Ko et al. 2005) and also shown in Table 2. The ADT was extracted from the torso images using the threshold method (Ko et al. 2010), as shown in Figure 2A. The threshold method is a sort of an imaging technique which uses the difference of the gray scale index from each tissue. Three-dimensional (3D) micro-CT images of the ADT were reconstructed and the volumes of the ADT were measured using Mimics 13.1 (Materialise N.V., Belgium). The total volume of the ADT was separated into the following subvolumes: total abdominal adipose tissue (TV), visceral abdominal adipose tissue (VV), and subcutaneous abdominal adipose tissue (SV).

The bone mineral density (BMD) and structural parameters of the trabecular and cortical bone were measured based on tibia images using CT-AN 1.10 (Skyscan N.V., Belgium), as depicted in Figure 3A. The structural parameters of the trabecular bone include the bone volume fraction (BV/TV,%), trabecular thickness (Tb.Th, mm), trabecular separation (Tb.Sp, mm), trabecular number (Tb.N, mm), trabecular bone pattern factor (Tb.Pf, mm), and structure model index (SMI) (Ko et al. 2005). BV/TV is the volume rate of the trabecular bone in the region of interest. Tb.Th is the average thickness of the trabecular bone. Tb.Sp is the average separation of the trabecular bone. Tb.N is the number of trabecular bones per unit length and Tb.Pf is the connectivity of the trabecular bone with a lower value indicating higher connectivity. SMI represents the morphological characteristics of the trabecular bone, with 0 indicating ideal for a plate-like structure, 3 indicating a rod-shaped structure, and 4 indicating a ball-shaped structure.

As shown in Figure 3A, the structural parameters of the cortical bone included bone volume (BV, mm^3), mean polar moment of inertia (MMI, mm), and cross-sectional thickness (Cs.Th, mm) (Ko et al. 2005). BV represents the volume of the cortical bone. MMI is the ability to resist shearing. Cs.Th is the cross-sectional thickness of the cortical bone. The length between the proximal and distal end of the tibia was measured from the images using Mimics 13.1. The growth plate (GP) was extracted from the tibia images, and 3D micro-CT images were reconstructed using Mimics 13.1. Subsequently, the volume of the growth plate (GV, mm^3) and thickness I, II of the growth plate (Gp.Th I, II) were also measured.

2.4. Statistical analysis

Analysis of covariance (ANCOVA) was performed to demonstrate the differences in TV, VV, SV, BMD and structural parameters of the tibia, length of tibia, GV, Gp.Th I, and Gp.Th II between the NOR and NS groups at six weeks using SPSS 12.0 (SPSS Inc., USA) ($p < 0.05$). All data are represented as the mean $\pm$ SE.

3. Results and discussion

In this study, we introduced circadian disturbances to growing male 129/sv mice by modulating LD cycles to simulate NSs (Figure 1A). To see whether biological rhythms function properly in these organisms, firstly we have examined two molecular markers related to generate and maintain circadian rhythms in mice, *Bmal1* and *Period2* genes. In good accordance with other studies (Bae et al. 2001; Akhtar et al. 2002), both mRNAs oscillate in a time-of-day specific manner, with

Table 2. The parameters used for scanning in the experiment.

Parameter	Pixel (μm)	Filter (mm)	Exposure time (msec)	Voltage (kV)	Ampere (μA)	Rotation (degree)
Tissue						
ADT	35	Al 1.0	790	100	100	1.2
Tibia	18	Al 1.0	2065	85	118	0.7

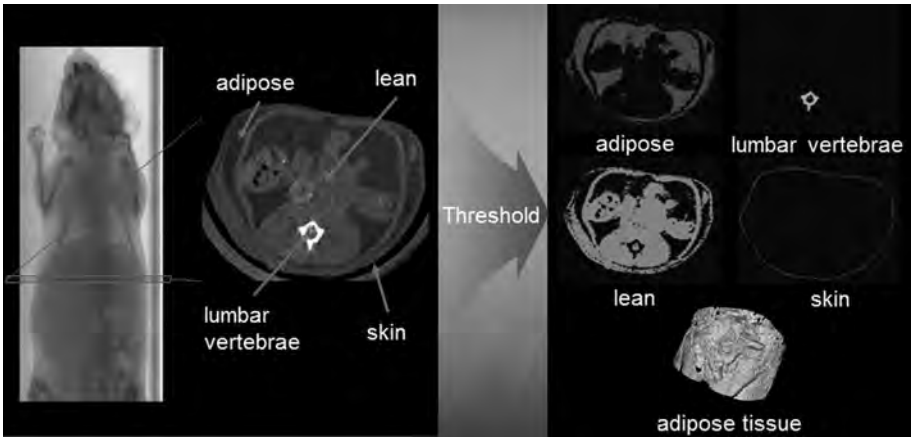

Figure 2. (A) A diagram of the body parts that are scanned by micro-computed tomography (micro-CT) is depicted on the left. The images are reconstructed by the threshold method and shown in colors on the right. (B) Three-dimensional micro-CT images of the abdominal adipose tissues (ADTs) taken at 0 and 6 weeks (wks) are shown. The yellow color represents the subcutaneous ADTs and the white color marks the visceral ADTs, respectively. It is evident that there are drastic changes in 3D morphological characteristics of the ADTs, especially in the visceral volumes of the NS group. (C) Quantitation of the volume of ADTs and the body weight over six weeks are shown as line graphs. TV: the volume of total abdominal adipose tissues; VV: the volume of visceral abdominal adipose tissues; SV: the volume of subcutaneous abdominal adipose tissues. All data are expressed as the mean $\pm$ SE. NS vs. NOR at 0–6 weeks, $^*p < 0.05$. While the SV and the weight and showed no significant difference between groups, the TV and the VV were significantly different between groups after six weeks ($^*p < 0.05$).

anti-phasic to each other, indicating these mice became synchronized well to LD cycles (Figure 1B).

We also have measured and evaluated the morphological characteristics of two peripheral tissues, ADTs, and tibiae in the organism and found that significant increase in the volumes of adipose tissues and alterations in tibia bones. Quantitative comparisons of the changes in the structural and morphological characteristics of the peripheral tissues of two groups at 0 week and 6 weeks are shown in Figures 2–4. The ADTs are related to various adult diseases, and bone plays a critical role in the structure of the body by providing support, enabling movement, and protecting the body from external stimuli (Akiyama et al. 1999; Ko et al. 2005; Zvonic et al. 2006; Francine et al. 2007). Alterations in these peripheral tissues greatly affect quality of life and contribute to associated health problems.

3.1. ADT and weight comparison

The changes in 3D morphological characteristics in each group are shown in Figure 2B. After six weeks, TV and VV in the NS group were significantly higher (69 and 92%, respectively) than those in the NOR group ($p < 0.05$) (Figure 2C top left and right). SV in the NS group was also slightly higher (23%) than that in the NOR group, but the difference was not significant (Figure 2C, bottom left). Both of the groups increased in their weight with no significant difference between groups at six weeks (Figure 2C, bottom right). It has been reported that the accumulation of ADT is closely related to cardiovascular and cerebrovascular disease and diabetes, and the diseases that were related are different to partial distribution of ADT (Wajchenberg 2000; Park and Kim 2003). The accumulation of VV is strongly related to metabolic syndrome and cardiovascular diseases, and SV has strong correlation with insulin sensitivity (Wajchenberg 2000; Park and Kim 2003). According to our results, VV was significantly increased by the disturbance in circadian rhythm. In this respect, it is important to note that some key regulators for energy metabolism, for instance, PGC-1α and AMP-activated protein kinase (AMPK), are strongly interconnected, under the regulation of circadian rhythms in mammals (Liu et al. 2007; Vieira et al. 2008; Lamia et al. 2009). Recently, Park et al. (2012) reported that when mice were exposed with different T cycles, either shortened or lengthened LD cycles, the disturbances could affect body weight and food intake. According to them, a shortened T cycle significantly increased the food intake of clock mutants and notably both T cycles could decrease the life span of wild type. Although the LD cycle manipulations and the parameters tested are quite different to our experiment, both clearly suggested that chronic circadian disturbances result in changes in physiology and health issues like obesity. Indeed, circadian clock genes oscillate within human adipocytes and alterations in clock gene expression are correlated with obesity (Bass and Takahashi 2010). Therefore, any disturbance on the rhythm may cause the malfunctioning of glucose and lipid metabolism that ends in metabolic disorders.

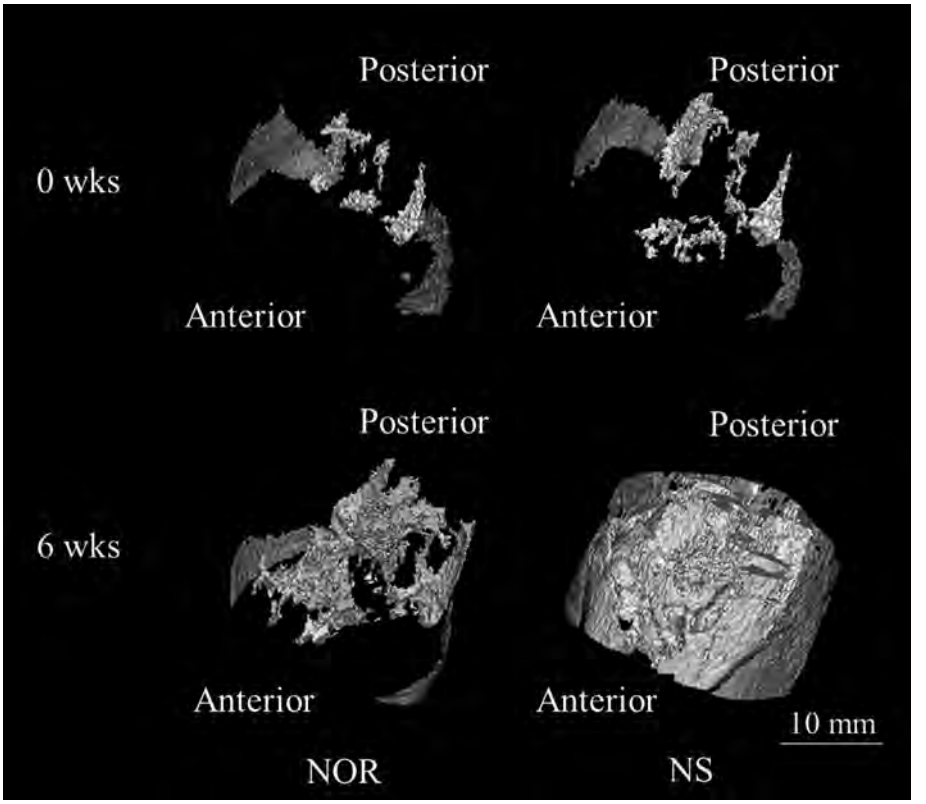

Figure 2. Continued.

3.2. Comparison of BMD and structural parameters

The changes in 3D morphological characteristics in each group are shown in Figure 3B. The BV, MMI, Cs.Th, and BMD were significantly lower (7, 13, 5, and 3%, respectively) in the NS group than in the NOR group at six weeks ($p < 0.05$) (Figure 3C). The BV/TV, Tb.Th, Tb.Sp, and Tb.N were lower (45, 4, 3, and 43%, respectively), and Tb.Pf and SMI were higher (12 and 3%, respectively) in the NS group than in the NOR group at six weeks, but the

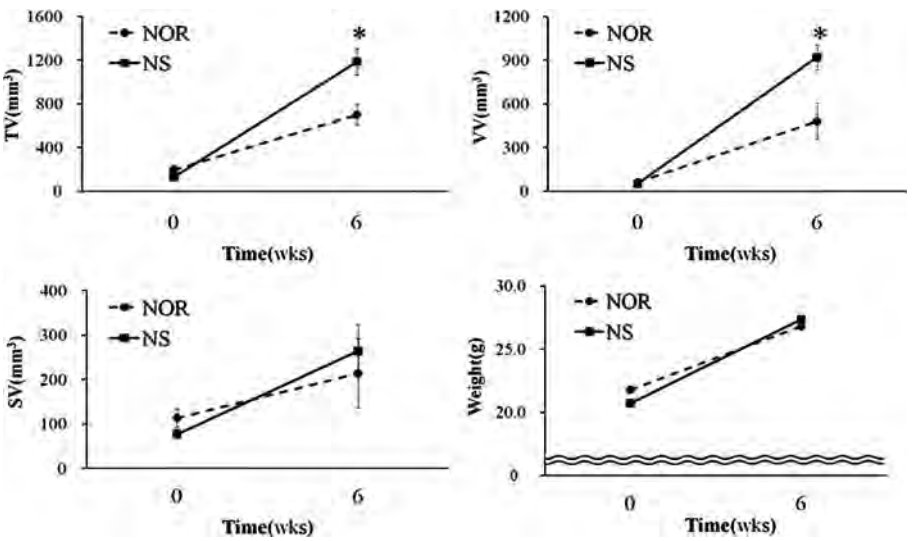

Figure 2. Continued.

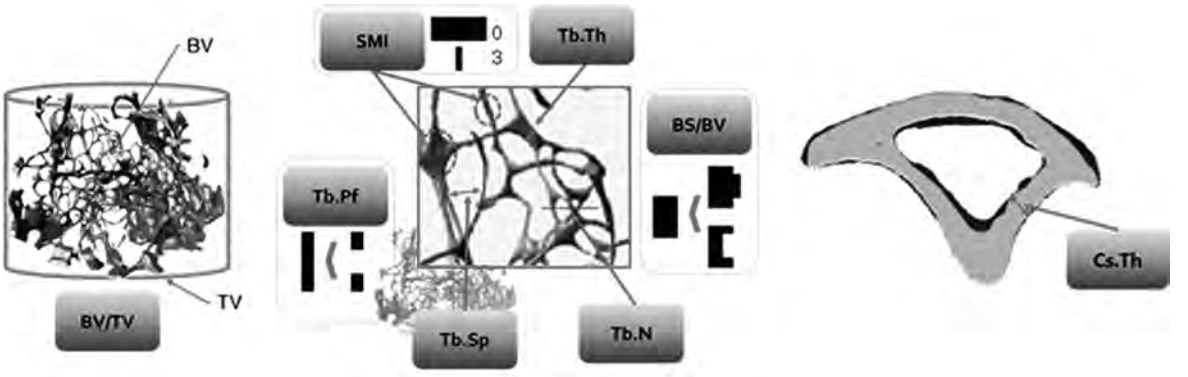

Figure 3. (A) The structural parameters of the trabecular (left and middle) and the cortical bone (right) measured in the experiment are depicted as diagrams adopted from Ko et al. (2005). Please see the text for the detailed description. (B) Representative 3D micro-computed tomography images of the cortical bone at 0 and 6 weeks. There were the changes in 3D morphological characteristics of the cortical bone in the NS group. (C) Changes in structural parameters (BV, MMI, Cs.Th) and BMD of the cortical bone over six weeks were quantified and shown in line graphs (mean $\pm$ SE, NS vs. NOR at 0–6 weeks, $^*p < 0.05$). All the structural parameters were significantly lower in the NS group than in the NOR group at six weeks.

differences were not significant. These results indicate that the volume of the cortical bone was smaller and the thickness of the cortical bone was thinner in the NS group than in the NOR group. We also detected weakening in MMI, which represents the ability to resist shearing. Thus, a disturbance in circadian rhythm appears to affect the morphological characteristics of the cortical bone of the tibia but does not seem to have an effect on the characteristics of the trabecular bone. The morphological characteristics of cortical bone are closely related to the strength of the bone (Ko et al. 2005). Therefore, disturbance in circadian rhythm in the NS group may result in an increase in the fractures risk mainly by decreasing the strength of the cortical bones.

3.3. Comparison of the GPs of the tibia

We also measured the length of the tibia, and the volume and thickness of the GP to evaluate how a disturbance in circadian rhythm affects the bone growth. Changes in the 3D morphological character-

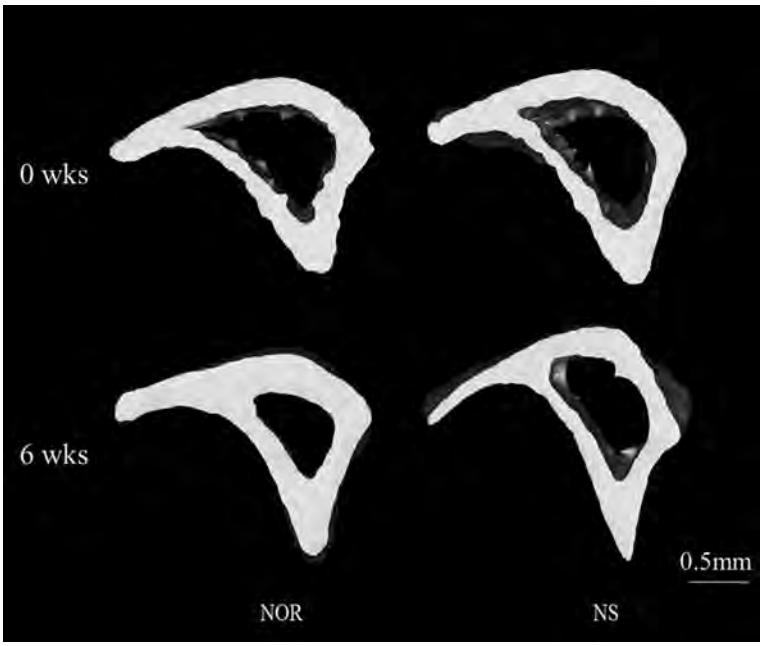

Figure 3. Continued.

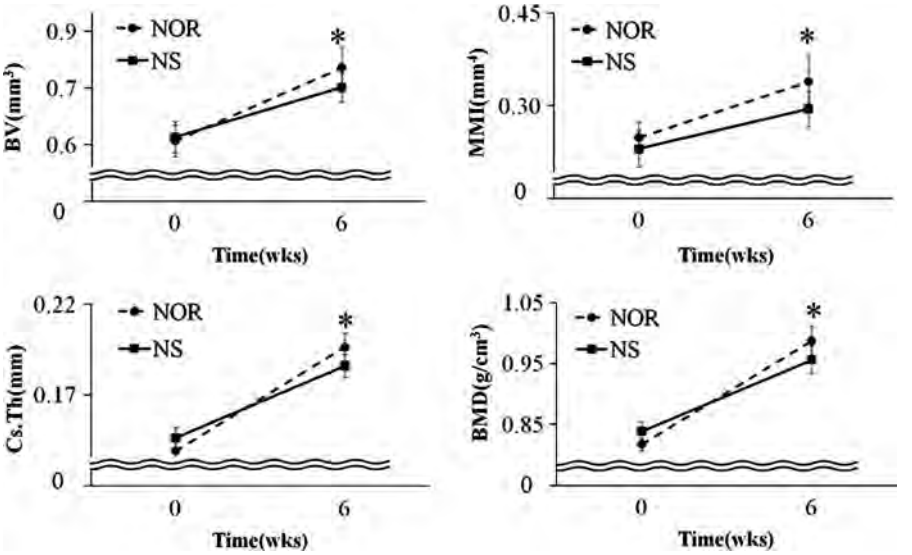

Figure 3. Continued.

istics in each group are shown in Figure 4A and B. The length of the tibia in the NS group was slightly shorter than that in the NOR group at six weeks. However, after six weeks, the GV, Gp.Th I, and Gp.Th II of the tibia were significantly lower (22, 20, and 20%, respectively) in the NS group than in the NOR group ($p < 0.05$) (Figure 4C). It is thus possible that a disturbance in circadian rhythm may be involved in the bone growth due to a decrease in the GP.

We used growing animals in the present study, so our results indicate that disturbances in circadian rhythm might induce a growth disability due to inhibition of adolescent growth, and increased adolescent obesity due to an increase in the accumulation of ADT,

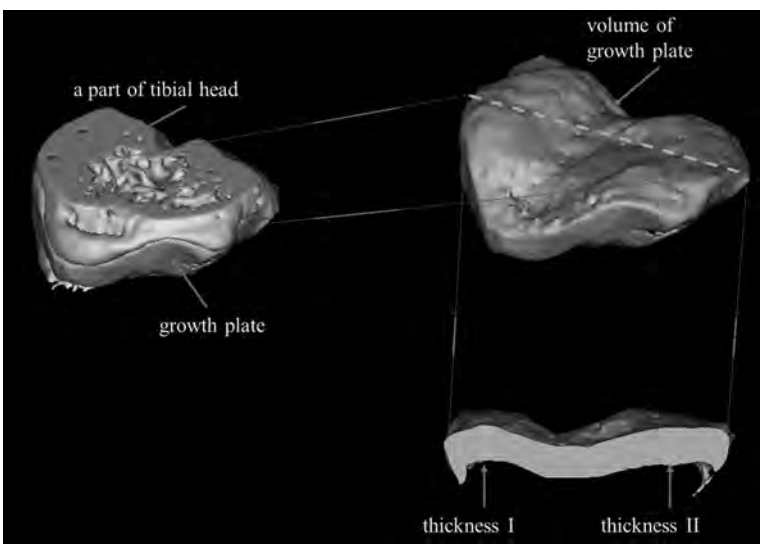

Figure 4. (A) The growth plates (GPs) were extracted from the tibiae and 3D images were reconstructed and the volume of the growth plate (GV, mm^3) and thickness I, II of the growth plate (Gp.Th I, II) were measured. (B) Representative 3D micro-computed tomography images of the GP of the tibiae from the NOR and the NS group at 0 and 6 weeks. Changes in 3D morphological characteristics of the GP, the volume (the first and second low) and the thickness (the third and fourth low), were more evident in the NS group. (C) Quantitation of the changes in the volume and thickness of the GP of the tibiae over six weeks are shown as line graphs (mean $\pm$ SE, NS vs. NOR at 0–6 weeks, $*p < 0.05$). The GV, Gp.Th I, and Gp.Th II were significantly lower in the NS group than in the NOR group at six weeks.

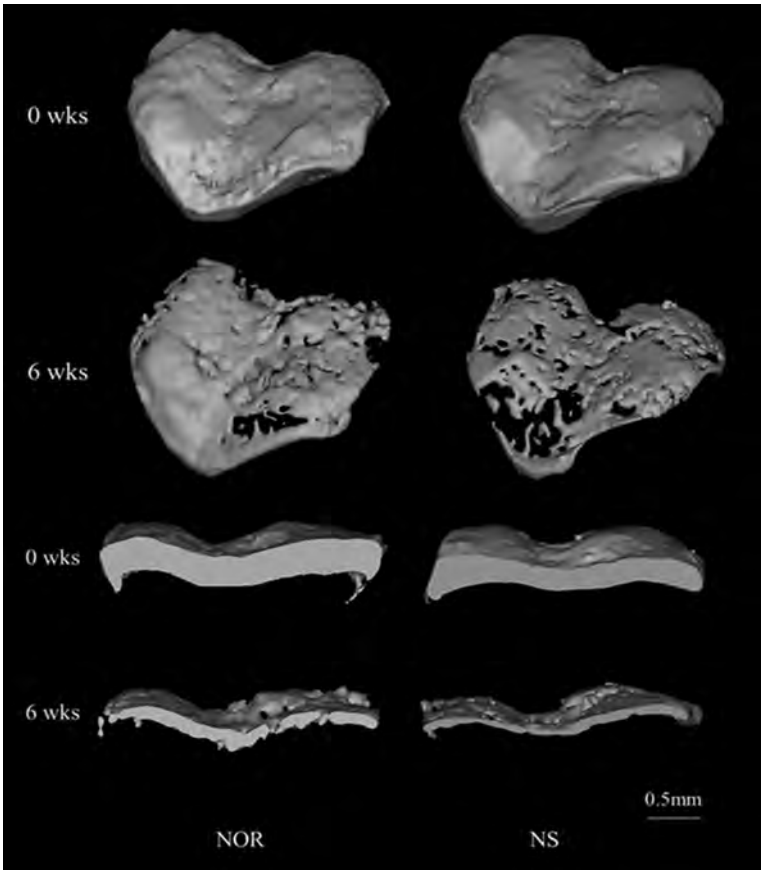

Figure 4. Continued.

especially visceral ADT, which leads to various metabolic disorders and cardiovascular disease.

In summary, our findings suggest that the disturbance in circadian rhythm induced by NSs could result in obesity due to an increased accumulation of ADT, an increased risk of bone fracture due to a weakening of the cortical bone, and also the inhibition of bone growth due to a reduction in the GP. Further studies

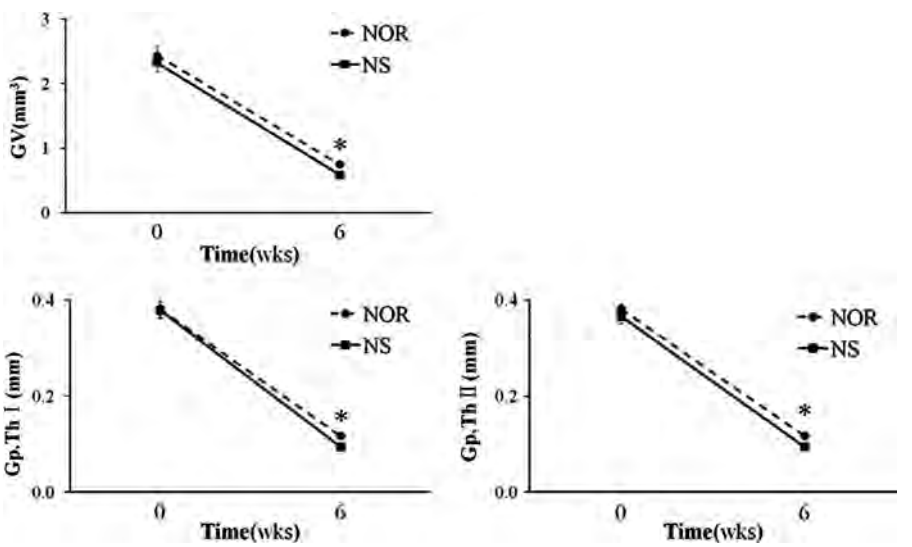

Figure 4. Continued.

with circadian mutant mice are under way to explore the molecular events those are responsible for the cortical bone growth and the accumulation of adipose tissues.

Acknowledgements

We are grateful to Dr Tack-Joong Kim, Jong-Bum Seo, and Michael Gelinsky for their valuable comments on this work. This research was supported by Leading Foreign Research Institute Recruitment Program through the National Research Foundation of Korea (NRF) funded by the Ministry of Education, Science and Technology (MEST) (201100263).

References

Akhtar RA, Reddy AB, Maywood ES, Clayton JD, King VM, Smith AG, Gant TW, Hastings MH, Kyriacou CP. 2002. Circadian cycling of the mouse liver transcriptome, as revealed by cDNA Microarray, is driven by the suprachiasmatic nucleus. Curr Biol. 12:540–550.

Akiyama M, Kouzu Y, Takahashi S, Wakamatsu H, Moriya T, Maetani M, Watabe S, Tei H, Sakaki Y, Shibata S. 1999. Inhibition of light- or glutamate-induced mPer1 expression represses the phase shifts into the mouse circadian locomotor and suprachiasmatic firing rhythms. J Neurosci. 19:1115–1121.

Bae K, Jin X, Maywood ES, Hastings MH, Reppert SM, Weaver DR. 2001. Differential functions of mPer1, mPer2 and mPer3 in the SCN circadian clock. Neuron. 30:525–536.

Bass J, Takahashi JS. 2010. Circadian integration of metabolism and energetics. Science. 330:1349–1354.

Bunger MK, Wilsbacher LD, Moran SM, Clendenin C, Radcliffe LA, Hogenesch JB, Simon MC, Takahashi JS, Bradfield CA. 2000. Mop3 is an essential component of the master circadian pacemaker in mammals. Cell. 103:1009–1017.

Francine OJ, Cermakian N, Boivin DB. 2007. Circadian rhythms of melatonin, cortisol, and clock gene expression during simulated night shift work. Sleep. 30:1427–1436.

Hastings MH, O'Neill JS, Maywood ES. 2007. Circadian clocks: regulators of endocrine and metabolic rhythms. J Endocrinol. 195:187–198.

Joo EY. 2006. Circadian neurobiology. Kor J Sleep Soc. 1: 1–5.

Ko C-Y, Seo D-H, Kim H-S. 2010. Suggestion of methodology for evaluation of abdominal adipose tissue of C57BL/6 female mice using in-vivo micro-CT. Tissue Eng Regen Med. 7:410–418.

Ko C-Y, Woo D-G, Kim H-S, Lee B-Y. 2005. Micro-CT evaluation in osteoporosis model. Kor J Phys Anthropol. 18:283–290.

Lamia KA, Sachdeva UM, DiTacchio L, Williams EC, Alvarez JG, Egan DF, Vasquez DS, Juguilon H, Panda S, Shaw RJ, et al. 2009. AMPK regulates the circadian clock by cryptochrome phosphorylation and degradation. Science. 326:437–440.

Lee SS, Kang CY, Kim DH. 2007. An evaluation of shift-worker's sleep and social life for the hospital workers. J Kor Soc Ind Sys Eng. 30:58–66.

Lee Y, Kim K. 2012. Posttranslational and epigenetic regulation of the CLOCK/BMAL1 complex in the mammalian. Anim Cells Syst. 16:1–10.

Liu C, Li S, Liu T, Borjigin J, Lin JD. 2007. Transcriptional coactivator PGC-1α integrates the mammalian clock and energy metabolism. Nature. 447:477–482.

Livak KJ, Schmittgen TD. 2001. Analysis of relative gene expression data using real-time quantitative PCR and the 2(-Delta Delta C(T)) method. Methods. 25:402–408.

Park N, Cheon S, Son GH, Cho S, Kim K. 2012. Chronic circadian disturbance by a shortened light-dark cycle increases mortality. Neurobiol Aging. 33:1122.e11–1122.e22.

Park SK, Kim EH. 2003. The effects of aerobic exercise on abdominal fat and leptin in obese adolescents. Kor J Orien Assoc Study Obes. 12:173–182.

Reppert SM, Weaver DR. 2001. Molecular analysis of mammalian circadian rhythms. Ann Rev Physiol. 63:647–676.

Robert Y, Moore MD. 1997. CIRCADIAN RHYTHMS: basic neurobiology and clinical applications. Ann Rev Med. 48:235–266.

Sun KH, Kim SP, Cho SH, Kim SJ, Cho NS, Kim DH, Son JR. 2009. Effect of sleep quality and health in emergency medical doctors on duty at night. J Kor Emerg Med Soc. 20:138–144.

Vieira E, Nilsson EC, Nerstedt A, Ormestad M, Long YC, Garcia-Roves PM, Zierath JR, Mahlapuu M. 2008. Relationship between AMPK and the transcriptional balance of clock-related genes in skeletal muscle. Am J Physiol Endocrinol Metab. 295:E1032–E1037.

Wajchenberg BL. 2000. Subcutaneous and visceral adipose tissue: their relation to the metabolic syndrome. Endocr Rev. 21:697–738.

Zvonic S, Ptitsyn AA, Conrad SA, Scott LK, Floyd ZE, Kilroy G, Wu X, Goh BC, Mynatt RL, Gimble JM. 2006. Characterization of peripheral circadian clocks in adipose tissues. Diabetes. 55:962–970.